



Radar Cross Section of Maritime Targets

Yannick Béniguel ⁽¹⁾, Philippe Pouliguen ⁽²⁾, and Gildas Kubické ⁽³⁾

(1) IEEA, Courbevoie, France

(2) DGA / AID, Paris, France

(3) DGA / MI, Bruz, France

Abstract

This paper resolves the issue of the radar cross-section computation of maritime targets in the HF domain. Two cases are thought of, up to a few hundreds of sailing miles, for the ground wave radar mode, and beyond several hundreds of sailing miles, depending on the ionosphere ionization level, for the skywave mode. The extra losses because of the swell event are incorporated for the ground wave case, assimilating the ocean surface to a rough surface.

1. Introduction

The detection of maritime targets has a developing interest, specifically for the coastal survey. This is a significant concern for France as the nation is the second on the planet for the degree of its exclusivity maritime zonal area. One approach to perform the survey is to use HF radars operating in the 3 – 30 MHz range. In this frequency range, two propagating modes exist together as the antenna radiates both a ground wave and a skywave. The objective for the skywave is that the antenna main lobe radiates with a low elevation angle. Therefore, the reflection on the lower ionosphere layers happens far away from the antenna and the reflected wave might reach the earth at more than 1,000 kilometers, even more if the ionosphere state permits completing several hops. These radars are Over the Horizon (OTH) radars. As a result, there is a blind zone for target detection from the antenna to the first point reached on the planet. The ground wave permits supplementing the detection range for distances up to a few hundreds of kilometers. This paper deals with the two propagation modes and aims to assess the radar cross section of a vessel for each one of these two modes.

2. HF Antenna pattern

We considered the case of HF antennas located in the air and near an infinite interface. This interface is between the air and the ground or the ocean, considered as a lossy medium. As an outcome, these antennas have two operating modes: a skywave and a ground wave mode. The calculation results presented in this paper have been obtained using the moment's method, addressing the electric and magnetic field integral equations (EFIE and

MFIE). To consider the ground interface, the Green's function has been modified, including additional terms permitting meeting the boundary equations on the interface plane. The Green's function turns into a 3 x 3 matrix and four cases, for the vertical and horizontal electric and magnetic dipoles shall be addressed. All terms of the corresponding equations include Sommerfeld integrals. For numerical implementation, the procedure used to address the Sommerfeld integrals is the complex image technique to get the impedance matrix of the radiating elements while it is the modified saddle point technique to get the far-field. Results obtained with the developed computer code [1] have been cross checked at the EDA radar cross section workshop [2].

Far-field computation: phase stationary technique

The modified saddle point technique is the preferred method for the far field computation as an analytical solution can be inferred. The integration is performed in the k_p complex plane. Equation (1) shows the value of the electric field vertical component radiated by a vertical electric dipole. The vertical dipoles carry the major contribution to this field component. Comparable equations, but with a lower level, are acquired for the other terms. A detailed derivation can be found in Collin [3] with as a final result for the scattered field:

$$j \frac{\omega \mu_0}{4 \pi} \left[\frac{e^{-j k_0 R_1}}{R_1} + R_{\square} \frac{e^{-j k_0 R_2}}{R_2} + \frac{e^{-j k_0 R_2}}{R_2} \frac{2 K \sqrt{K} e^{-j \pi / 4}}{(\lambda_p \sqrt{\sin \vartheta})} \sqrt{\frac{w_p}{k_0}} F \left(\lambda_p \sqrt{\frac{k_0 R_2}{2}} \right) \right] \quad (1)$$

With R_{\square} the Fresnel reflection coefficient on the lossy interface and F is the Sommerfeld attenuation function. R_1 and R_2 are the distances between the source dipole and its image to the observation point. $K = n^2$ and n is the lossy medium index. w_p and λ_p are the pole locations in the k_p complex plane and in the steepest descent contour complex plane.

The field transmitted by the structure in (1) is the sum of three terms: the direct field, the reflected field multiplied by the Fresnel reflection coefficient, and a third term which peaks on the interface and represents the ground wave. On

the ground plane (the ocean surface), $\vartheta = \pi/2$ and the Fresnel reflection coefficient is equal to -1 . The initial two terms collapse and are left with the ground wave assimilated in what follows to a creeping wave.

2.1 Creeping wave attenuation in the lit region

The lit region is the region where for an observation point it exists both a direct and a reflected ray transmitted by the structure. It is consequently up to the distance of the horizon. Beyond this distance, the first and second terms in (1) are absent and just remaining the third term. Based on the altitude of source points above sea level, a sensible choice of the horizon distance, characterizing the lit region boundary, is 10 sailing miles (18 km).

2.2 Creeping wave attenuation in the shadow region

The air–ocean interface is assimilated to a smooth convex surface and we calculate the propagation of the creeping wave using a uniform asymptotic method. We consider the case where both the starting point, named Q' , and the observation point, named Q , are located on the surface (cf Figure 1). The launching point corresponds to the lit region boundary and the observation point to the radar location.

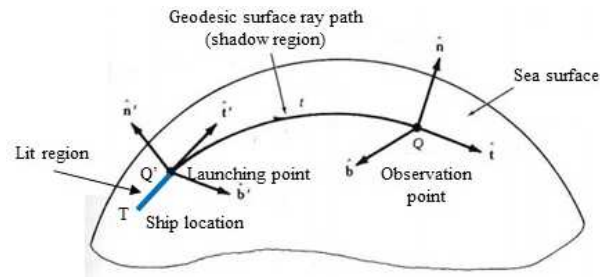


Figure 1: Creeping wave propagation on a smooth convex surface

The starting coefficient is given by the third term of (1). Adding all contributions from the various dipoles on the vessel illuminated by a unitary plane wave incident field, we obtain the value of the equivalent magnetic source dipole, named p_m , at point Q . The standard parameters m (the Fock parameter) and ξ are used in the following calculation. They are defined as

$$m(\tau) = \left(\frac{k a_0(\tau)}{2} \right)^{1/3}; \quad \xi = \int_{\tau(Q')}^{\tau(Q)} \frac{m(\tau)}{a_0(\tau)} d\tau \quad (2)$$

τ is the coordinate of a point along the geodesic line from Q to Q' on the earth assimilated to a sphere of constant radius $a_0(\tau) = a$ where a is the earth radius.

For a perfectly conducting surface, the transmitted field at point Q is given by the equation (3) simplified in the case of propagation over a sphere. A more elaborated expression can be found in [4]. The function $\tilde{V}(\xi)$ is the generalized Fock function in the considered case of a vertically polarized electric field (h case in the usual notations).

$$dE_m(Q | Q') = \frac{-j k}{4 \pi} dp_m(Q') \frac{e^{-j k t}}{t} \left\{ 2 \hat{b}' \cdot \hat{n} \left(1 - \frac{j}{k t} \right) \tilde{V}(\xi) \right\} \quad (3)$$

with b' the unit vector tangent to the surface at point Q' and opposite to the geodesic line. n is the normal to the surface at point Q . t is the path length along the geodesic line. It is consequently an arc length over the earth's surface.

The term between brackets in (3) corresponds to the shadow region attenuation function. It is displayed in figure 2 presented hereafter.

2.3 The sea as a lossy medium

The results presented in the beyond section, including the Fock scattering function, were obtained considering the ocean as a perfect conductor (PC). The Fock function $\tilde{V}(\xi)$ given in (3) can be written as a series of propagating modes, quickly merging. Every mode relates to a residue in the estimation of the integral. Very few of them are generally needed to get an accurate solution. The related propagation constants are, depending on the wave polarization, the zeros of the Airy function (TE case), or of its derivative (TM case). Considering the propagation over a non-zero surface impedance interface modifies the attenuation coefficients. For the considered TM case, they are obtained from the solutions of the following equations [5]:

$$Ai'(-\alpha_n) - j m \zeta e^{-j \pi/3} Ai(-\alpha_n) = 0 \quad (4)$$

with Ai the Airy function. The propagation constants are given by

$$\Omega = m \alpha_n e^{j \pi/6} / a = \alpha_n \xi e^{j \pi/6} \quad (5)$$

with $\zeta = Z_s / Z_0$ and Z_s is the impedance of the conducting medium.

There is an infinite number of zeros for these two functions. For a null surface impedance, the zeros of equation (4) are those of the Airy derivative function while for an infinite impedance they are those of the Airy function. Increasing the value of the surface impedance, beginning from zero for the perfectly conducting case, will move the zeros values towards higher values and accordingly, increment the propagation losses.

For the sea electrical constants previously considered and a frequency of 10 MHz, we obtain $Z_{s0} = (2.822, 2.797)$ and $\zeta_0 = (7.48 \cdot 10^{-3}, 7.42 \cdot 10^{-3})$. Solving equation (4) with these values, we obtain the new propagation coefficients: $\alpha_n = (1.6167, 3.5014, 4.9979, \dots)$.

2.4 Taking the swell into account

The extra losses because of the swell can be assessed using a similar methodology. The swell is assumed to be stationary. Under this hypothesis, a relationship can be

derived to relate the wave's height RMS to the wind strength. The sea surface is then assimilated to a rough surface and we look for a modification of the surface impedance to consider the swell. This derivation has been done by Barrick [6]. To get the amplitude and period of the wave, the Neumann-Pierson spectrum has been used. The angle between the wave's bearing and the line of sight is a datum in this calculation. It is considered in the spectrum formula. The standardized impedance is then obtained by the equation:

$$\bar{\zeta} = \zeta_0 + \frac{1}{4} \int_{-\infty}^{\infty} \int_{-\infty}^{\infty} F(p, q) W(p, q, \beta) dp dq \quad (6)$$

with W the sea spectrum, β the angle between the wave's direction and the line of sight, and F the function related to the roughness contribution. $\bar{\zeta}$ and ζ_0 are the normalized impedances with and without wind.

Equation (4) has been solved at frequency 10 MHz for the related impedance values for the three cases: no wind, a sea state 4 and a sea state 6. The corresponding shift of the initial zero of the Airy function derivative is displayed in table 1.

Table 1: the first zero of the Airy function derivative depending on the sea state at 10 MHz

Wind strength	1st zero of $Ai'(-x)$
Perfectly Conducting (PC) surface	1.0188
ocean surface (no wind)	1.6167
ocean surface (Beaufort 4)	1.6869
ocean surface (Beaufort 6)	1.8744

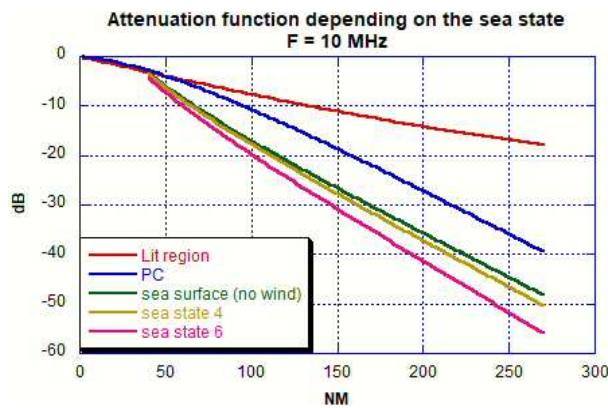


Figure 2: propagation losses due to the earth curvature and to the swell

The extra losses for the attenuation function are displayed on figure 2. The lit region corresponds to a flat earth. Beyond a value of around 50 sailing miles, broadens the deep shadow region. The development that was used for this calculation is valid in this region. The plot shows the differences obtained by approximating the ocean to a perfect conductor and considering the swell. At a distance of 200 NM, there is around a 10 dB difference between the PC case and the genuine case and 5 dB more for an ocean state equivalent to 6. The surface impedance results apply outside the transition region corresponding to values of the

ξ variable greater than 1. Hence, the last three curves on the right plot of figure 4 begin at abscissa $\xi = 1$.

2.5 Ground wave RCS

The ground wave radar cross section is given by the third term of equation (1). It is estimated at the target location, with respect to an isolated target aside from that the problem incorporates the ocean considered as a lossy medium. Both the emerged and immersed components of the vessel are modeled in the calculation. At the target location, the Sommerfeld attenuation function is equal to 1. Just remaining the $1/R_2$ dependency on the distance at this location. The total field is obtained by adding the contributions of all vertical and horizontal dipoles located above and beneath the ocean level. To get the signal at a given distance, the got value shall be diminished by two factors corresponding to the distance between the source and the observation point and to the creeping wave attenuation function.

- Distance source – observation point

In the lit region, the radiated field decreases with the distance, named R_2 in (1), from the ship to the observation point. The arc length and the chord are indistinguishable for this small distance. In the shadow region, it has a dependency on the arc length on the earth's surface, named t in (3). Adding the various terms contributing to the scattered field at a given observation point, along the arc distance will be held.

- Creeping wave attenuation function

Two cases have been identified for the creeping wave attenuation function: one for the lit region and one for the shadow region. The lit region attenuation function applies till the horizon (around 10 NM). The corresponding attenuation is weak, regularly under 1 dB for this distance. The shadow region attenuation function then, at that point, applies. The relating losses increase significantly, especially in the deep shadow region and on the swell event.

3. Skywave RCS

The GISM model [7] allows computing rays' trajectories between the antenna and the boat after reflection in the ionosphere. GISM has been created by IEEA under a contract with the European Space Agency (ESA) to appraise ionosphere bias and scintillation, at first in the L band, for navigation systems purposes. The ability to address the HF band has been added subsequently for radar survey applications.

Inputs to the ray's trajectories calculation are the electron density and the terrestrial magnetic field at any point and any time in space. The ray's trajectories are determined solving the Haselgrove differential equations. This is done with a Runge Kutta algorithm.

As an example, we have considered a mid-latitude link with the observer and the target located at a similar latitude and a toward the west propagation. The f10.7 solar flux index, which plays a major role in the ionization level, was set to 165, corresponding to a peak of the solar activity. The electron density map shows an F-layer peak at around 350 km for the time considered for this simulation: 12:00 UT. In this example, the rays displayed on the figure are launched from the antenna location with an elevation angle increasing with a 1° step angle. The first point reached in that case is situated 751 km away from the antenna.

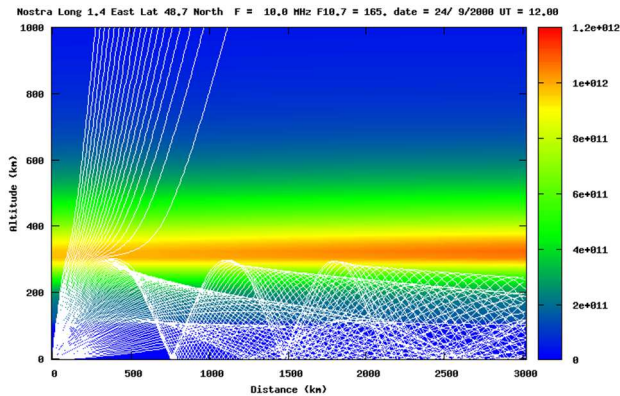


Figure 3: ray's trajectories for a mid latitude link

The operating frequency was set to 10 MHz in this simulation. The rays are reflected or transmitted depending on the ray elevation angle at the launching point. Two altitudes of reflection corresponding to two caustics of reflected rays for the D and E ionosphere layers are observable on the plot. To estimate a budget link for each one of the rays, this shall in addition be multiplied by the antenna gain for the elevation angle considered.

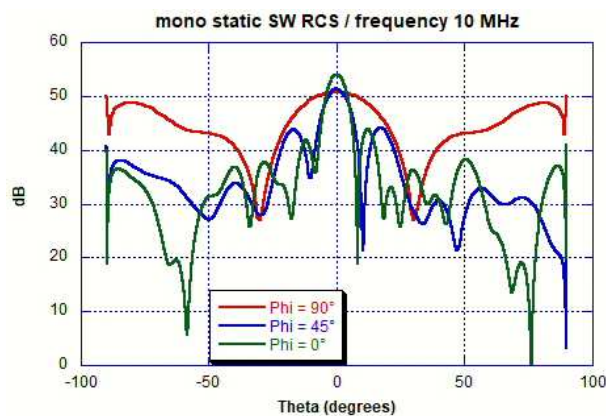


Figure 4: The two components of the skywave (SW) and the ground wave (GW) in three azimuthal planes. The z-axis (perpendicular to the interface) is taken as a reference for the zenith angle.

The Skywave RCS of a ship is calculated using the first two terms of (1). We have considered a 110 meters long vessel and three azimuthal planes: 0°, 45° and 90° with respect to the bearing axis. The obtained results are shown on Figure 4. The structure being symmetrical regarding the roll axis,

this symmetry can likewise be noticed for the transverse azimuthal plane (the red curve). The peak values got are about the same for the three cases with, all things considered, maximum values for the transverse incidence corresponding to the greatest coupling. To be noticed, the ground wave RCS value, with a comparable level, in the horizontal plane ($\vartheta = \pm 90^\circ$).

4. Conclusion

The calculation of the radar cross-section of a maritime target has been introduced for the two HF propagation modes: the ground wave and the skywave. The calculation performed permits isolating the respective contributions and resolving the two issues separately.

The ground wave RCS calculation has been decomposed into two sections: one for the lit region from the target to the horizon and one for the shadow region. The two solutions perfectly match in the transition region. At a distant point the received signal corresponds to the RCS, decreased by the propagation losses along the geodesic line from the target to the observation point, in addition to losses due to the creeping wave attenuation. The additional losses due to the swell are included in this calculation, assimilating the swell on the ocean surface, to a rough surface.

The sky wave radar calculation is performed similarly. It was shown the continuity between the two results at grazing angle values. The sky wave propagation path is gotten by a ray technique calculation showing the occurrence of two caustic surfaces corresponding to a reflection at the D and E layers altitudes.

References

- [1] <http://www.icea.fr/fr/logiciels/icare-mom.html>
- [2] European Defense Agency (EDA) workshop, Brussels, November 2019
- [3] R. E. Collin, "Hertzian dipole radiation over a lossy earth or sea: some early and late 20th-century controversies", IEEE Antennas and Propagation Magazine, Vol 46, N° 2, April 2004
- [4] P. Pathak, "Techniques for high frequency problems", Antenna Handbook, chapter 4, Van Nostrand, 1988
- [5] G. L. James, "Geometrical theory of diffraction for electromagnetic waves", Peter Peregrinus Ltd, 1986
- [6] Barrick D., "Theory of Ground wave propagation across a rough sea at decameter wavelengths", 1970
- [7] Y. Béniguel, P. Hamel, "A Global Ionosphere Scintillation Propagation Model for Equatorial Regions", Journal of Space Weather Space Climate, 1, (2011), doi: 10.1051/swsc/2011004